



Lee Jacklick, RMI

Chapter 7

Marshall Islands

7.1 Climate Summary

7.1.1 Current Climate

- Warming trends are evident in both annual and half-year mean air temperatures at Majuro (southern Marshall Islands) since 1955 and at Kwajalein (northern Marshall Islands) since 1952.
- The frequency of Warm Days has increased while the number of Cool Nights has decreased at both Majuro and Kwajalein. These temperature trends are consistent with global warming.
- At Majuro, a decreasing trend in annual rainfall is evident since 1954. This implies either a shift in the mean location of the Inter-Tropical Convergence Zone (ITCZ) away from Majuro and/or a change in the intensity of rainfall associated with the ITCZ. There has also been a decrease in the number of Very Wet Days since 1953. The remaining annual, seasonal and extreme rainfall trends at Majuro and Kwajalein show little change.
- Tropical cyclones (typhoons) affect the Marshall Islands mainly between June and November. An average of 22 cyclones per decade developed within or crossed the Marshall Islands Exclusive Economic Zone (EEZ) between the 1977 and 2011 seasons. Tropical cyclones were most frequent in El Niño years (50 cyclones per decade) and least frequent in La Niña years (3 cyclones per decade). Thirteen of the 71 tropical cyclones (18%) between the 1981/82 and 2010/11 seasons became severe events (Category 3 or stronger) in the Marshall Islands EEZ. Available data are not suitable for assessing long-term trends.
- Wind-waves in the Marshall Islands are influenced by trade winds seasonally, and the El Niño–Southern Oscillation (ENSO) interannually. Wave heights are greater in December–March than June–September. Available data are not suitable for assessing long-term trends (see Section 1.3).

7.1.2 Climate Projections

For the period to 2100, the latest global climate model (GCM) projections and climate science findings indicate:

- El Niño and La Niña events will continue to occur in the future (*very high confidence*), but there is little consensus on whether these events will change in intensity or frequency;
- Annual mean temperatures and extremely high daily temperatures will continue to rise (*very high confidence*);
- Average rainfall is projected to increase (*high confidence*), along with more extreme rain events (*high confidence*);
- Droughts are projected to decline in frequency (*medium confidence*);
- Ocean acidification is expected to continue (*very high confidence*);
- The risk of coral bleaching will increase in the future (*very high confidence*);
- Sea level will continue to rise (*very high confidence*); and
- Wave height is projected to decrease in the dry season (*low confidence*) and wave direction may become more variable in the wet season (*low confidence*).

7.2 Data Availability

There are currently nine operational observation stations in the Marshall Islands. Multiple observations within a 24-hour period are taken at Majuro, Utirik, Ailinglaplap, Jaluit, Wotje, Mili, Amata Kabua International Airport and Kwajalein, and single daily observations at Laura and Arno. The primary meteorological stations are located at Majuro (the capital) on the southern end of the Ratak chain and at Kwajalein near the centre of the Ralik chain. Observations began at Majuro in 1951 and at Kwajalein in 1945.

Majuro rainfall from 1954 and air temperature from 1955, and Kwajalein rainfall from 1945 and air temperature from 1949 (daily values from 1953), have been used in this report. Both records are homogeneous. Additional information on historical climate trends in the Marshall Islands region can be found in the Pacific Climate Change Data Portal www.bom.gov.au/climate/pccsp/.

Wind-wave data from buoys are particularly sparse in the Pacific region, with very short records. Model and reanalysis data are therefore required to detail the wind-wave climate of the region. Reanalysis surface wind data have been used to drive a wave model over the period 1979–2009 to generate a hindcast of the historical wind-wave climate.

7.3 Seasonal Cycles

Information on temperature and rainfall seasonal cycles can be found in Australian Bureau of Meteorology and CSIRO (2011).

7.3.1 Wind-driven Waves

Surface wind-wave driven processes can impact on many aspects of Pacific Island coastal environments, including: coastal flooding during storm wave events; coastal erosion, both during episodic storm events and due to long-term changes in integrated wave climate; characterisation of reef morphology and marine habitat/species distribution; flushing and circulation of lagoons; and potential shipping and renewable wave energy solutions. The surface offshore wind-wave climate can be described by characteristic wave heights, lengths or periods, and directions.

The wind-wave climate of the Marshall Islands shows spatial variability between the northern and southern Islands.

In the south (e.g. on the south-east coast of Majuro), the wave climate is characterised by trade wind generated waves from the north-east and

south-east. A northerly component of swell propagated from storm events in the north Pacific is observed in December–March, with swell from Southern Ocean storms in June–September. Some southerly waves which may be associated with cyclones are also observed. Waves are directed from the north-east during the northern trade months of December–March, have greater wave heights than the annual mean (mean around 4'8" (1.4 m), and slightly shorter periods (mean 7.8 s) (Figure 7.1). During the wetter months June–September, waves are directed mostly from the east and south-east, have smaller heights (mean 3'8" (1.1 m)) and slightly longer periods than the annual mean (mean 8.5 s) (Table 7.1). Waves larger than 6'9" (2.1 m) (99th percentile) at Majuro occur predominantly during December–March directed from north-east to south, with some large long-period northerly and north-easterly waves observed, associated with extra-tropical storms. The height of a 1-in-50 year wave event to the southeast of Majuro is calculated to be 12'0" (3.7 m).

In the north (e.g. on the sheltered east coast of Kwajalein), waves are characterised by variability of the

Northern Hemisphere trade winds. During June–September waves at Kwajalein are locally generated in the east and have increasing period through the season (mean around 7.6 s) and lower than average wave heights (mean 2'10" (0.9 m)), with southerly swell waves associated with Southern Ocean storms (Figure 7.2). In December–March waves are north-easterly and have a fairly stable monthly mean period (mean around 7.5 s) and greater than average heights (mean around 4'3" (1.3 m) (Table 7.1). These waves consist of local trade wind generated waves, and some swell generated by northern extra-tropical storms and cyclones to the south. Waves larger than 6'6" (2.0 m) (99th percentile) occur mostly during the dry months (December–March) from around the east due to trade winds, with large easterly and south-westerly waves in other months. Large waves are seen from all directions in November caused by tropical cyclones and extra-tropical storms, with some long period waves greater than 10 s. The height of a 1-in-50 year wave event at the east coast of Kwajalein is calculated to be 16'6" (5.0 m).

No suitable dataset is available to assess long-term historical trends in the Marshall Islands wave climate. However, interannual variability may be assessed in the hindcast data. The wind-wave climate displays strong interannual variability at both Majuro and Kwajalein, varying with the El

Niño–Southern Oscillation (ENSO). During La Niña years, wave power is greater than during El Niño years in June–September at both locations. Waves are directed more strongly from the east year round near Majuro in La Niña years, and from the east rather than south-east in June–September at

Kwajalein with no change in direction in December–March in La Niña years. The location of the Inter-Tropical Convergence Zone (ITCZ) can also have an impact in this area, reducing locally generated wind waves.

Table 7.1: Mean wave height, period and direction from which the waves are travelling around the Marshall Islands in December–March and June–September. Observation (hindcast) and climate model simulation mean values are given with the 5–95th percentile range (in brackets). Historical model simulation values are given for comparison with projections (see Section 7.5.6 – Wind-driven waves, and Tables 7.8 and 7.9). A compass relating number of degrees to cardinal points (direction) is shown.

		Hindcast Reference Data (1979–2009), Kwajalein (northern Marshall Islands)	Climate Model Simulations (1986–2005) (northern Marshall Islands)	Hindcast Reference Data (1979–2009), Majuro, (southern Marshall Islands)	Climate Model Simulations (1986–2005) (southern Marshall Islands)
Mean wave height (feet)	December–March	4.3 (2.8–5.9)	8.0 (6.8–9.2)	4.7 (3.3–6.3)	6.9 (5.6–8.3)
	June–September	2.8 (1.8–4.1)	4.0 (3.3–4.9)	3.7 (2.6–4.9)	3.8 (3.2–4.7)
Wave Period (seconds)	December–March	7.5 (6.3–9.4)	8.2 (7.6–9.0)	7.8 (6.4–10.3)	8.0 (7.3–8.9)
	June–September	7.6 (6.0–9.8)	7.1 (6.2–8.0)	8.5 (6.6–10.6)	7.4 (6.5–8.2)
Wave direction (degrees clockwise from North)	December–March	60 (40–80)	50 (40–70)	60 (30–100)	50 (40–60)
	June–September	110 (70–200)	90 (70–120)	130 (90–180)	100 (80–140)

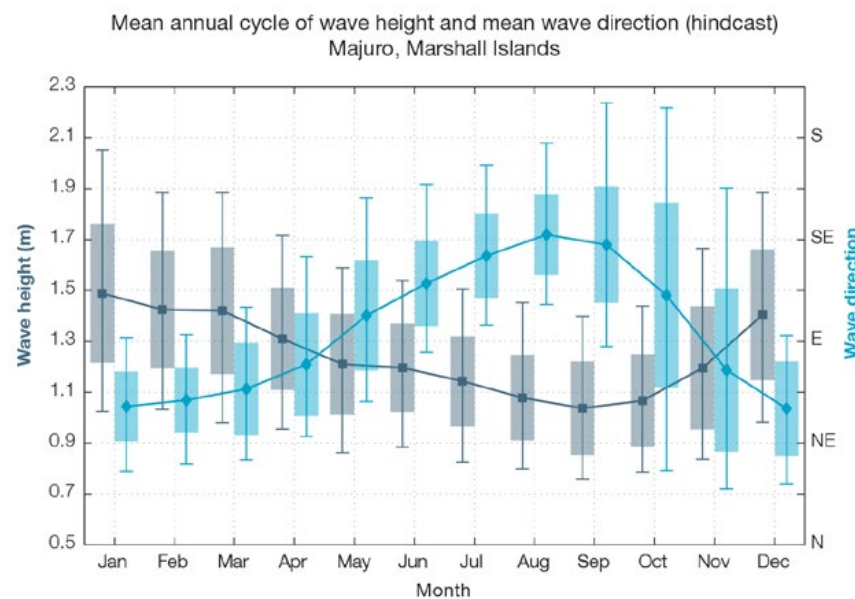


Figure 7.1: Mean annual cycle of wave height (grey) and mean wave direction (blue) on the south-east coast of Majuro in hindcast data (1979–2009). To give an indication of interannual variability of the monthly means of the hindcast data, shaded boxes show 1 standard deviation around the monthly means, and error bars show the 5–95% range. The direction from which the waves are travelling is shown (not the direction towards which they are travelling).

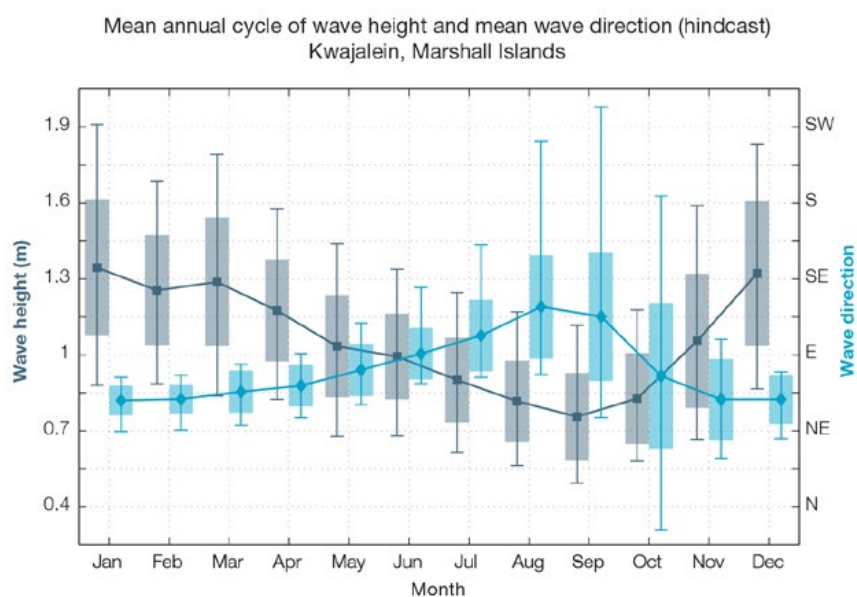


Figure 7.2: Mean annual cycle of wave height (grey) and mean wave direction (blue) on the sheltered east coast of Kwajalein in hindcast data (1979–2009). To give an indication of interannual variability of the monthly means of the hindcast data, shaded boxes show 1 standard deviation around the monthly means, and error bars show the 5–95% range. The direction from which the waves are travelling is shown (not the direction towards which they are travelling).

7.4 Observed Trends

7.4.1 Air Temperature

Annual and Half-year Mean Air Temperature

Warming trends in annual and half-year mean temperatures at Majuro since 1955 and Kwajalein since 1949 are statistically significant at the 5% level (Figure 7.3, Figure 7.4 and Table 7.2). Maximum and minimum temperature trends at Kwajalein are much stronger compared to Majuro. The warming temperature trends at both sites are consistent with global warming trends.

Extreme Daily Air Temperature

Warming trends are also evident in extreme daily temperatures with the number of Warm Days increasing and Cool Nights decreasing at both Majuro and Kwajalein (Figure 7.5, Table 7.3). Warm Nights have also increased at Majuro. All of these trends are statistically significant. The remainder of the extreme daily temperature trends presented in Table 7.3 are not statistically significant.

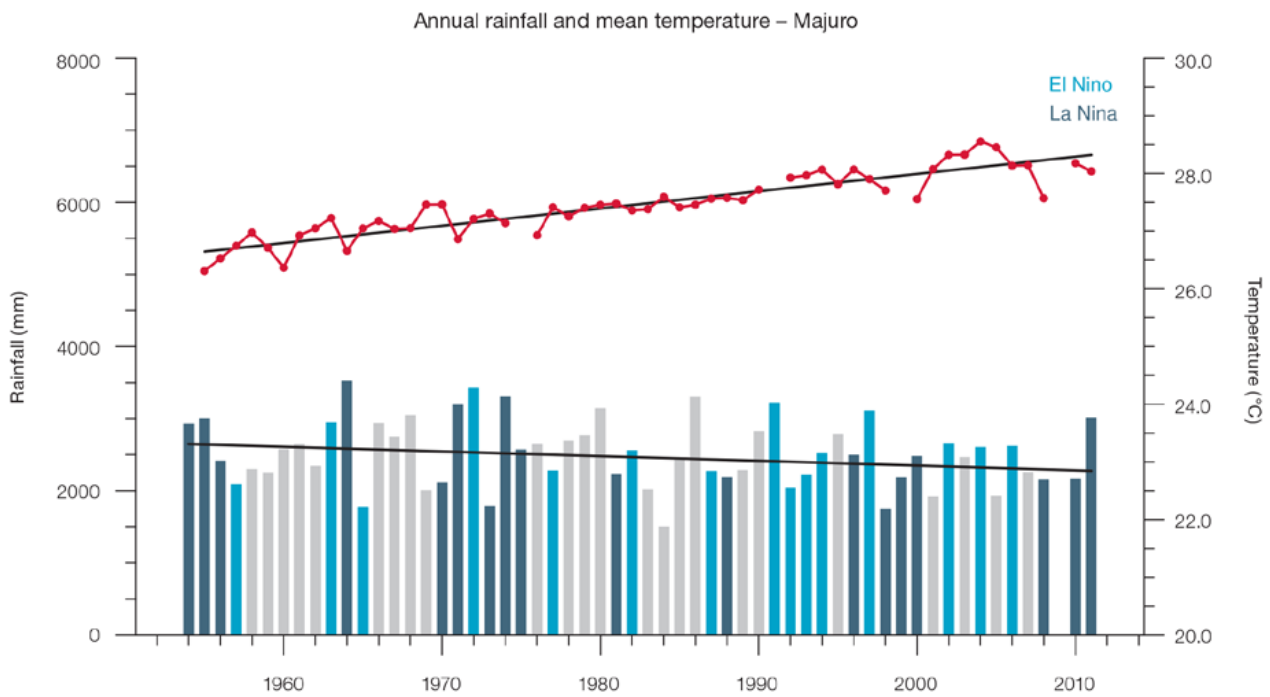


Figure 7.3: Observed time series of annual average values of mean air temperature (red dots and line) and total rainfall (bars) at Majuro. Light blue, dark blue and grey bars denote El Niño, La Niña and neutral years respectively. Solid black trend lines indicate a least squares fit.

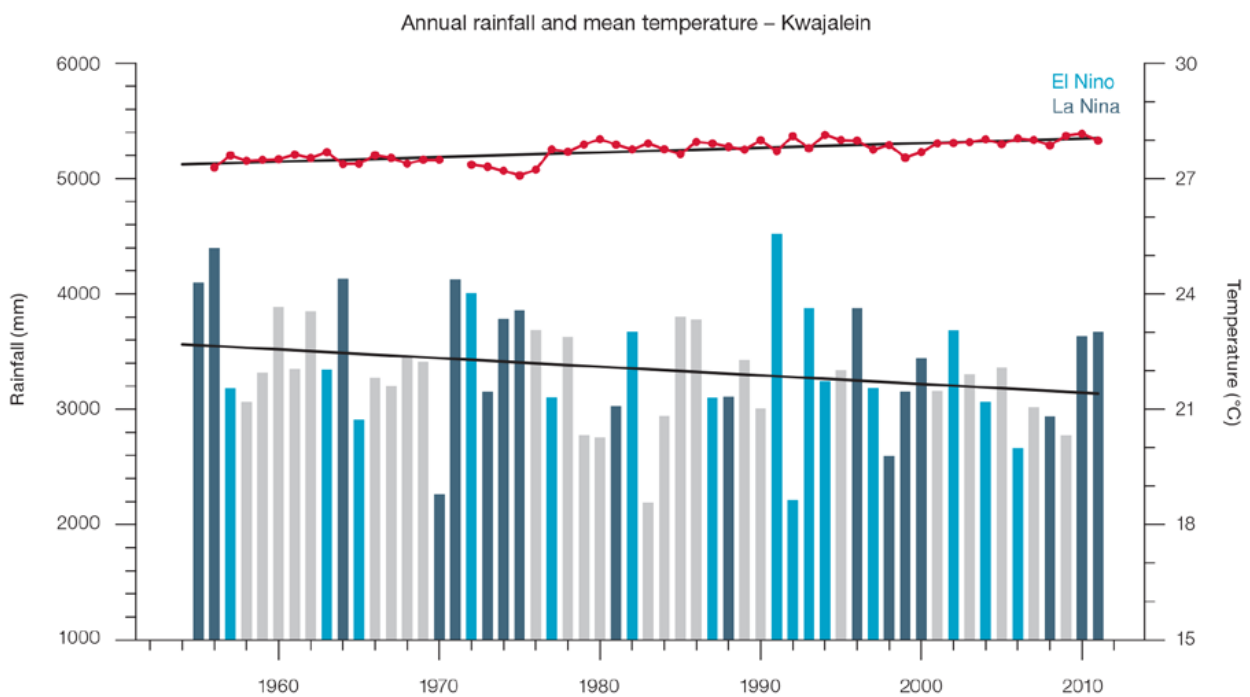


Figure 7.4: Observed time series of annual average values of mean air temperature (red dots and line) and total rainfall (bars) at Kwajalein. Light blue, dark blue and grey bars denote El Niño, La Niña and neutral years respectively. Solid black trend lines indicate a least squares fit.

Table 7.2: Annual and half-year trends in air temperature (Tmax, Tmin, Tmean) and rainfall at Majuro (top) and Kwajalein (bottom). The 95% confidence intervals are shown in brackets. Values for trends significant at the 5% level are shown in **boldface**.

Majuro	Tmax °F/10yrs [°C/10yrs]	Tmin °F/10yrs [°C/10yrs] 1955–2011	Tmean °F/10yrs [°C/10yrs]	Rain inches/10yrs [mm/10yrs] 1954–2011
Annual	+0.18 (+0.02, +0.31) [+0.10] (+0.01, +0.17])	+0.23 (+0.15, +0.31) [+0.13] (+0.08, +0.17])	+0.21 (+0.11, +0.29) [+0.12] (+0.06, +0.16])	-3.05 (-6.33, -0.02) [-77.4] (-160.7, -0.5])
Nov–Apr	+0.06 (-0.23, +0.40) [+0.03 (-0.13, +0.22)]	+0.21 (+0.14, +0.30) [+0.12] (+0.08, +0.17])	+0.16 (+0.02, +0.32) [+0.09] (+0.01, +0.18])	-0.97 (-3.80, +1.52) [-24.6 (-96.4, +38.6)]
May–Oct	+0.21 (+0.08, +0.32) [+0.12] (+0.05, +0.18])	+0.23 (+0.09, +0.38) [+0.13] (+0.05, +0.21])	+0.22 (+0.14, +0.30) [+0.12] (+0.08, +0.17])	-1.78 (-3.77, +0.32) [-45.1 (-95.7, +8.1)]

Kwajalein	Tmax °F/10yrs [°C/10yrs]	Tmin °F/10yrs [°C/10yrs] 1949–2011	Tmean °F/10yrs [°C/10yrs]	Rain inches/10yrs [mm/10yrs] 1945–2011
Annual	+0.49 (+0.35, +0.65) [+0.27] (+0.19, +0.36])	+0.48 (+0.38, +0.58) [+0.27] (+0.21, +0.32])	+0.53 (+0.44, +0.60) [+0.30] (+0.24, +0.33])	-1.19 (-3.80, +1.36) [-30.4 (-96.5, +34.6)]
Nov–Apr	+0.46 (+0.26, +0.67) [+0.26] (+0.15, +0.37])	+0.45 (+0.31, +0.56) [+0.25] (+0.17, +0.31])	+0.44 (+0.31, +0.59) [+0.24] (+0.17, +0.33])	-0.22 (-1.73, +1.11) [-5.5 (-44.0, +28.3)]
May–Oct	+0.65 (+0.48, +0.78) [+0.36] (+0.27, +0.43])	+0.51 (+0.43, +0.58) [+0.28] (+0.24, +0.32])	+0.58 (+0.49, +0.66) [+0.32] (+0.27, +0.37])	-1.03 (-2.56, +0.51) [-26.1 (-65.0, +12.9)]

Table 7.3: Annual trends in air temperature and rainfall extremes at Majuro and Kwajalein. The 95% confidence intervals are shown in parentheses. Values for trends significant at the 5% level are shown in **boldface**.

		Majuro	Kwajalein
TEMPERATURE		1956–2011	1953–2011
Warm Days (days/decade)		+3.94 (+2.02, +5.61)	+6.21 (-8.79, +23.89)
Warm Nights (days/decade)		+9.61 (+5.12, +16.06)	+8.24 (-1.19, +17.58)
Cool Days (days/decade)		-3.31 (-6.88, +0.75)	-18.50 (-44.97, +0.39)
Cool Nights (days/decade)		-6.77 (-11.21, -3.36)	-12.08 (-18.44, -7.78)
RAINFALL		1955–2011	1953–2011
Rain Days ≥ 1 mm	(days/decade)	-1.11 (-4.29, +1.84)	-1.71 (-4.85, +1.67)
Very Wet Day rainfall	(inches/decade)	-2.30 (-4.52, -0.16)	-0.74 (-2.54, +1.22)
	(mm/decade)	-58.44 (-114.75, -4.00)	-18.70 (-64.57, +31.00)
Consecutive Dry Days (days/decade)		-0.36 (-0.94, 0.00)	0.00 (-0.91, +0.43)
Max 1-day rainfall	(inches/decade)	-0.04 (-0.29, +0.19)	-0.02 (-0.22, +0.16)
	(mm/decade)	-0.98 (-7.45, +4.73)	-0.56 (-5.63, +4.04)

Warm Days: Number of days with maximum temperature greater than the 90th percentile for the base period 1971–2000
 Warm Nights: Number of days with minimum temperature greater than the 90th percentile for the base period 1971–2000
 Cool Days: Number of days with maximum temperature less than the 10th percentile for the base period 1971–2000
 Cool Nights: Number of days with minimum temperature less than the 10th percentile for the base period 1971–2000
 Rain Days ≥ 1 mm: Annual count of days where rainfall is greater or equal to 1 mm (0.039 inches)
 Very Wet Day rainfall: Amount of rain in a year where daily rainfall is greater than the 95th percentile for the reference period 1971–2000
 Consecutive Dry Days: Maximum number of consecutive days in a year with rainfall less than 1 mm (0.039 inches)
 Max 1-day rainfall: Annual maximum 1-day rainfall

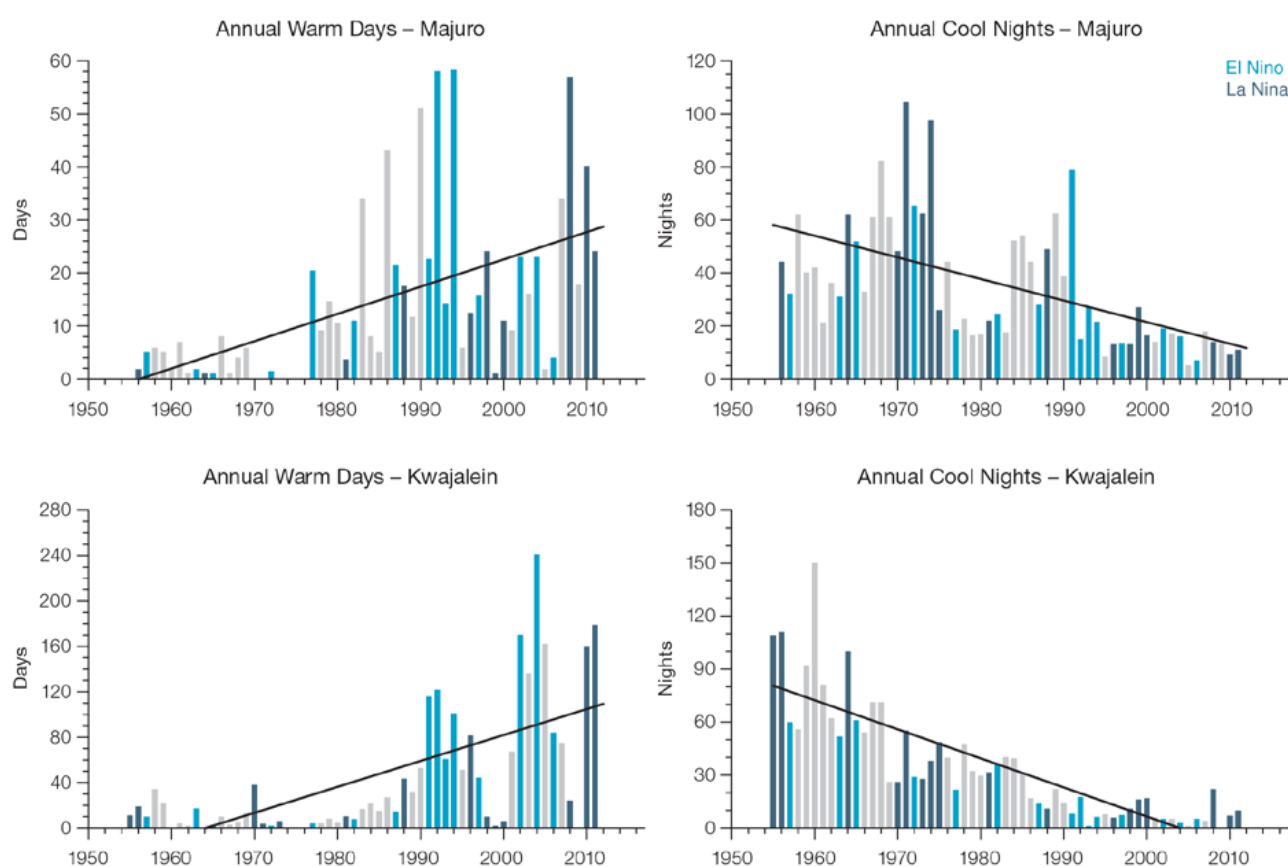


Figure 7.5: Observed time series of annual total number of Warm Days at Majuro (top left panel) and Kwajalein (bottom left panel), and annual Cool Nights at Majuro (top right panel) and Kwajalein (bottom right panel). Solid black trend lines indicate a least squares fit.

7.4.2 Rainfall

Annual and Half-year Total Rainfall

Notable interannual variability associated with the ENSO is evident in the observed rainfall records for Majuro since 1954 (Figure 7.3) and Kwajalein since 1945 (Figure 7.4). The negative trend in Majuro annual rainfall (Table 7.2) is statistically significant at the 5% level. This implies either a shift in the mean location of the Inter-Tropical Convergence Zone or a change in the intensity of rainfall associated with the ITCZ. The ITCZ is closest to the equator in March–May, and furthest north during September–November, when it becomes broader, expanding both to the north and south.

The other total rainfall trends presented in Table 7.2 and Figure 7.4 are not statistically significant. In other words, excluding Majuro annual rainfall, the other trends show little change at Majuro and Kwajalein.

Daily Rainfall

Daily rainfall trends for Majuro and Kwajalein are presented in Table 7.3. Figure 7.6 shows trends in annual Very Wet Days and Rain Days ≥ 1 mm (days with rainfall) at Majuro and Kwajalein. The negative trend in Majuro annual Very Wet Day rainfall is statistically significant. The other daily rainfall trends in Table 7.3 are not significant.

7.4.3 Tropical Cyclones

When tropical cyclones (typhoons) affect the Marshall Islands they tend to do so between June and November.

The tropical cyclone archive of the Northern Hemisphere indicates that between the 1977 and 2011 seasons, 78 tropical cyclones developed within or crossed the Marshall Islands EEZ. This represents an average of 22 cyclones per decade. Refer to Chapter 1, Section 1.4.2 (Tropical Cyclones) for an explanation of the difference in the number of tropical cyclones occurring in the Marshall Islands in this report (Australian Bureau of Meteorology and CSIRO, 2014) compared to Australian Bureau of Meteorology and CSIRO (2011). The interannual variability in the number of tropical cyclones in the Marshall Islands EEZ is large, ranging from zero in some seasons to 11 in 1997 (Figure 7.7).

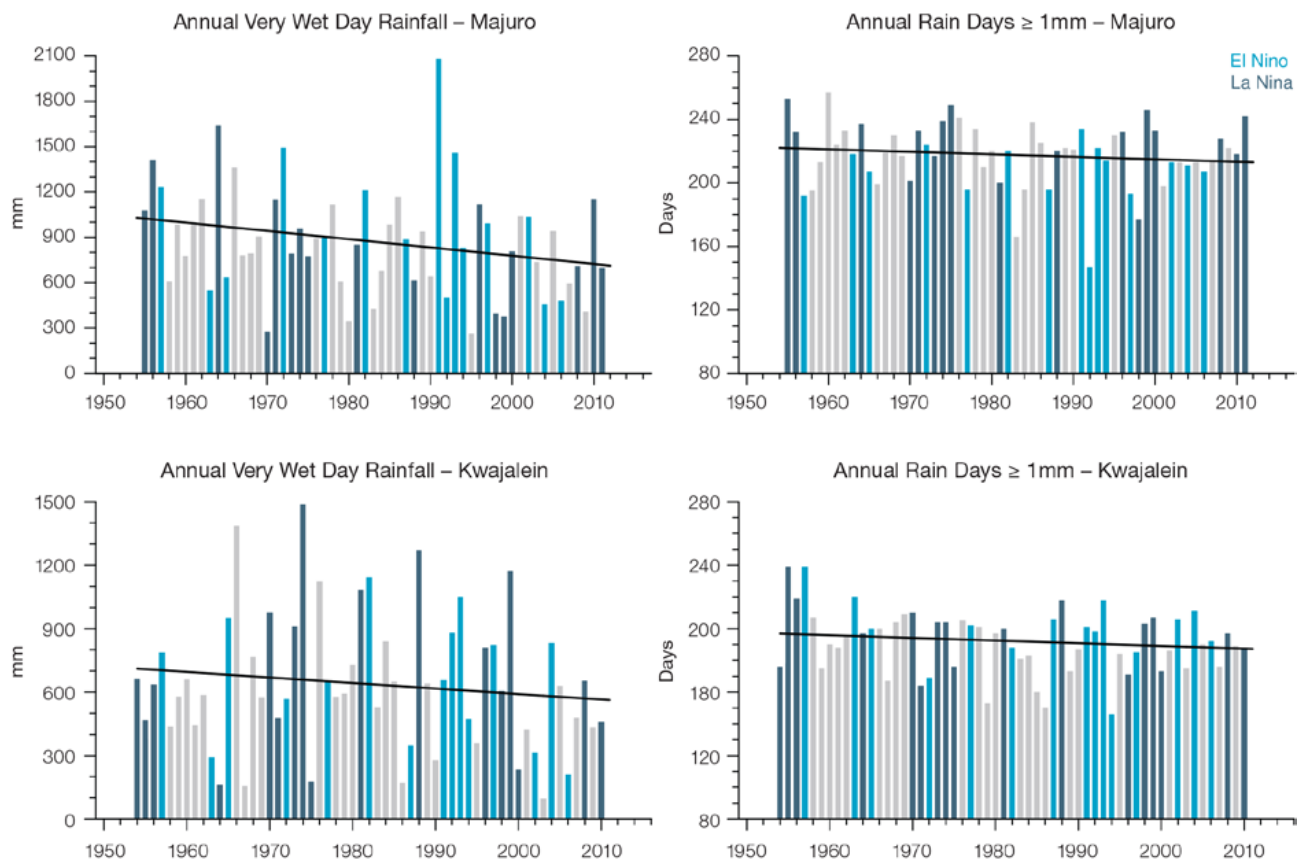


Figure 7.6: Observed time series of annual total values of Very Wet Days at Majuro (top left panel) and Kwajalein (bottom right panel), and annual Rain Days ≥ 1 mm at Majuro (top right panel) and Kwajalein (bottom right panel). Solid black trend lines indicate a least squares fit.

Tropical cyclones were most frequent in El Niño years (50 cyclones per decade) and least frequent in La Niña years (3 cyclones per decade). The neutral season average is 18 cyclones per decade. Thirteen of the 71 tropical cyclones (18%) between the 1981/82 and 2010/11 seasons became severe events (Category 3 or stronger) in the Marshall Islands EEZ.

Long term trends in frequency and intensity have not been presented as country scale assessment is not recommended. Some tropical cyclone tracks analysed in this subsection include the tropical depression stage (sustained winds less than or equal to 34 knots) before and/or after tropical cyclone formation.

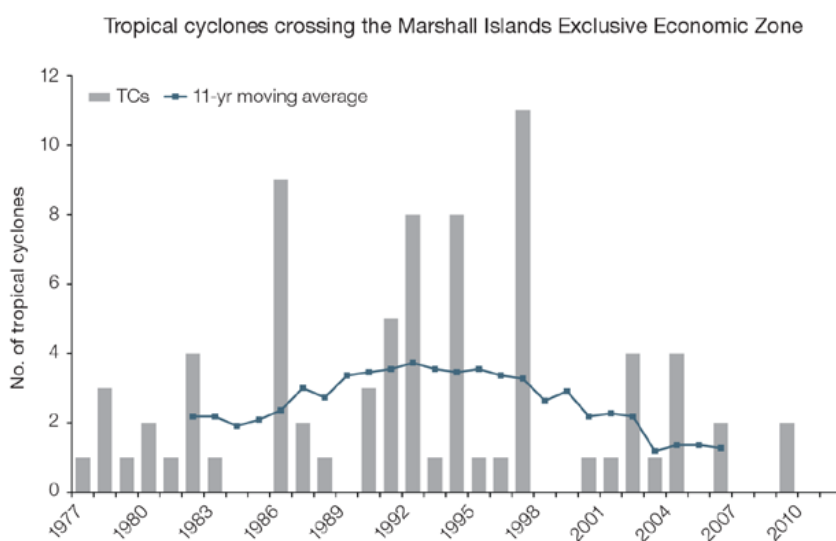


Figure 7.7: Time series of the observed number of tropical cyclones developing within and crossing the Marshall Islands EEZ per season. The 11-year moving average is in blue.

7.5 Climate Projections

The performance of the available Coupled Model Intercomparison Project (Phase 5) (CMIP5) climate models over the Pacific has been rigorously assessed (Brown et al., 2013a, b; Grose et al., 2014; Widlansky et al., 2013). The simulation of the key processes and features for the Marshall Islands region is similar to the previous generation of CMIP3 models, with all the same strengths and many of the same weaknesses. The best-performing CMIP5 models used here have lower biases (differences between the simulated and observed climate data) than the best CMIP3 models, and there are fewer poorly-performing models. For the Marshall Islands, the most important model bias is that the simulated rainfall in the ITCZ in the present day is too strong, particularly in the northern part of the Marshall Islands. This affects the confidence in the model projections. Out of 27 models assessed, one model was rejected for use in these

projections due to biases in the mean climate. Climate projections have been derived from up to 26 new GCMs in the CMIP5 database (the exact number is different for each scenario, Appendix A), compared with up to 18 models in the CMIP3 database reported in Australian Bureau of Meteorology and CSIRO (2011).

It is important to realise that the models used give different projections under the same scenario. This means there is not a single projected future for the Marshall Islands, but rather a range of possible futures for each emission scenario. This range is described below.

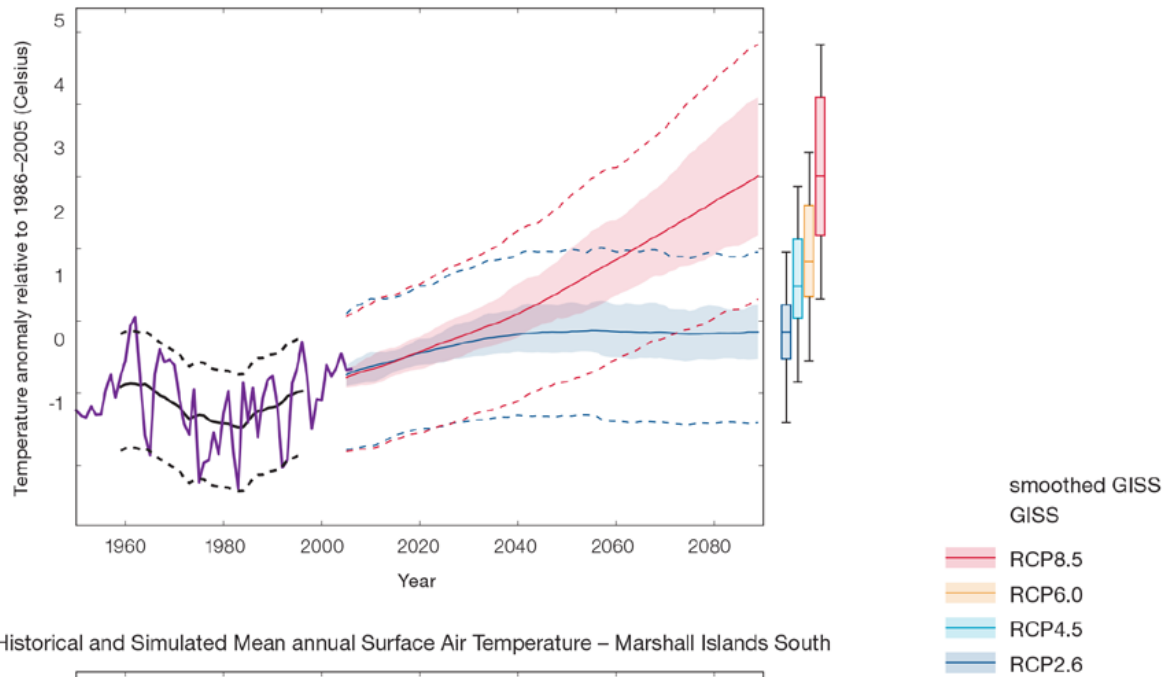
7.5.1 Temperature

Further warming is expected over the northern and southern Marshall Islands (Figure 7.8, Tables 7.6 and 7.7). Under all RCPs, the warming is up to 1.1°C by 2030, relative to 1995, but after

2030 there is a growing difference in warming between each RCP.

For example, in the northern Marshall Islands by 2090, a warming of 2.2 to 4.2°C is projected for RCP8.5 (very high emissions) while a warming of 0.5 to 1.2°C is projected for RCP2.6 (very low emissions), with a similar range in the southern Marshall Islands. This range is broader than that presented in Australian Bureau of Meteorology and CSIRO (2011) because a wider range of emissions scenarios is considered. While relatively warm and cool years and decades will still occur due to natural variability, there is projected to be more warm years and decades on average in a warmer climate.

Historical and Simulated Mean annual Surface Air Temperature – Marshall Islands North



Historical and Simulated Mean annual Surface Air Temperature – Marshall Islands South

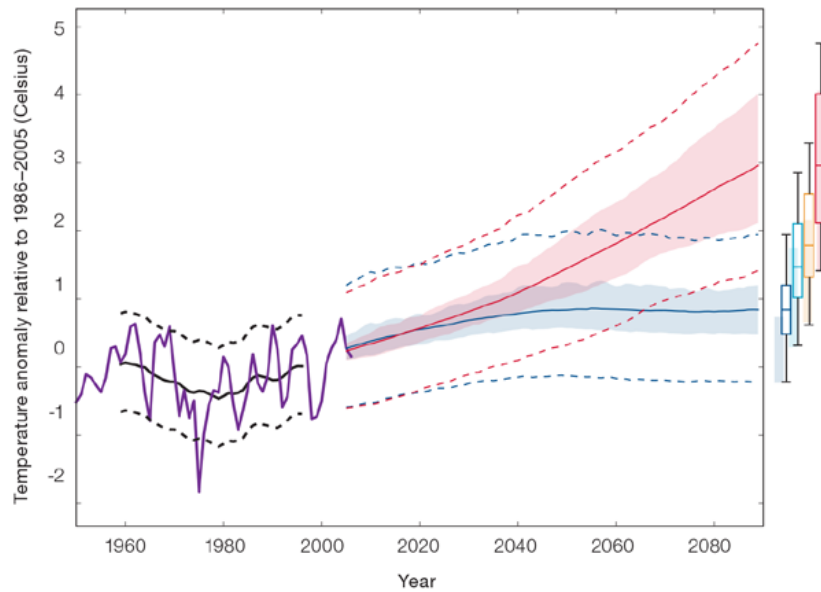


Figure 7.8: Historical and simulated surface air temperature time series for the region surrounding the northern (top) and southern (bottom) Marshall Islands. The graph shows the anomaly (from the base period 1986–2005) in surface air temperature from observations (the GISS dataset, in purple), and for the CMIP5 models under the very high (RCP8.5, in red) and very low (RCP2.6, in blue) emissions scenarios. The solid red and blue lines show the smoothed (20-year running average) multi-model mean anomaly in surface air temperature, while shading represents the spread of model values (5–95th percentile). The dashed lines show the 5–95th percentile of the observed interannual variability for the observed period (in black) and added to the projections as a visual guide (in red and blue). This indicates that future surface air temperature could be above or below the projected long-term averages due to interannual variability. The ranges of projections for a 20-year period centred on 2090 are shown by the bars on the right for RCP8.5, 6.0, 4.5 and 2.6.

There is *very high confidence* that temperatures will rise because:

- It is known from theory and observations that an increase in greenhouse gases will lead to a warming of the atmosphere; and
- Climate models agree that the long-term average temperature will rise.

There is *medium confidence* in the model average temperature change shown in Tables 7.6 and 7.7 because:

- The new models do not match temperature changes in the recent past in the Marshall Islands as well as in other places, possibly due to problems with the observed records or with the models; and
- There is a bias in the simulation of sea-surface temperatures and the ITCZ in this region, affecting the uncertainty the projections of rainfall but also temperature.

7.5.2 Rainfall

The long-term average rainfall in the northern and southern Marshall Islands is projected by almost all models to increase. The increase is greater for the higher emissions scenarios, especially towards the end of the century (Figure 7.9, Tables 7.6 and 7.7). Most models project an increase in rainfall in both the wet and dry seasons. The year-to-year rainfall variability over Marshall Islands is much larger than the projected change, except in the upper range of models in the highest emission scenario by 2090 (Figure 7.9). There will still be wet and dry years and decades due to natural variability, but most models show that the long-term average is expected to be wetter. The effect of climate change on average rainfall may not be obvious in the short or medium term due to natural variability. These projections are similar to those in Australian Bureau of Meteorology and CSIRO (2011).

There is general agreement between models that rainfall will increase. However the bias in the ITCZ intensity in the models lowers the confidence of the magnitude of the projected changes. The 5–95th percentile range of projected values from CMIP5 climate models is large, e.g. for example in the northern Marshall Islands in RCP8.5 (very high emissions) the range is -5 to +7% by 2030 and -2 to 46% by 2090.

There is *high confidence* that the long-term rainfall over Marshall Islands will increase because:

- The majority of CMIP3 and CMIP5 models agree that the rainfall in the ITCZ will increase under a warmer climate; and
- There are well-understood physical reasons why a warmer climate will lead to increased rainfall in the ITCZ region.

There is *medium confidence* in the model average rainfall change shown in Tables 7.6 and 7.7 because:

- The complex set of processes involved in tropical rainfall is challenging to simulate in models. This means that the confidence in the projection of rainfall is generally lower than for other variables such as temperature;
- The new CMIP5 models broadly simulate the influence from the key features such as the Inter-Tropical Convergence Zone, but have some uncertainty and biases, similar to the old CMIP3 models;
- The future behaviour of the ENSO is unclear, and the ENSO strongly influences year-to-year rainfall variability; and
- The CMIP5 models are similar to the previous CMIP3 models in overestimating the present average rainfall of Marshall Islands.

7.5.3 Extremes

Extreme Temperature

The temperature on extremely hot days is projected to increase by about the same amount as average temperature. This conclusion is based on analysis of daily temperature data from a subset of CMIP5 models (Chapter 1). The frequency of extremely hot days is also expected to increase.

For the northern Marshall Islands the temperature of the 1-in-20-year hot day is projected to increase by approximately 0.7°C by 2030 under the RCP2.6 (very low) scenario and by 0.8°C under the RCP8.5 (very high) scenario. By 2090 the projected increase is 0.8°C for RCP2.6 (very low) and 3.3°C for RCP8.5 (very high).

For the southern Marshall Islands the temperature of the 1-in-20-year hot day is projected to increase by approximately 0.7°C by 2030 under the RCP2.6 (very low) scenario and by 0.8°C under the RCP8.5 (very high) scenario. By 2090 the projected increase is 0.8°C for RCP2.6 (very low) and 3.1°C for RCP8.5 (very high).

There is *very high confidence* that the temperature of extremely hot days and the temperature of extremely cool days will increase, because:

- A change in the range of temperatures, including the extremes, is physically consistent with rising greenhouse gas concentrations;
- This is consistent with observed changes in extreme temperatures around the world over recent decades; and
- All the CMIP5 models agree on an increase in the frequency and intensity of extremely hot days and a decrease in the frequency and intensity of cool days.

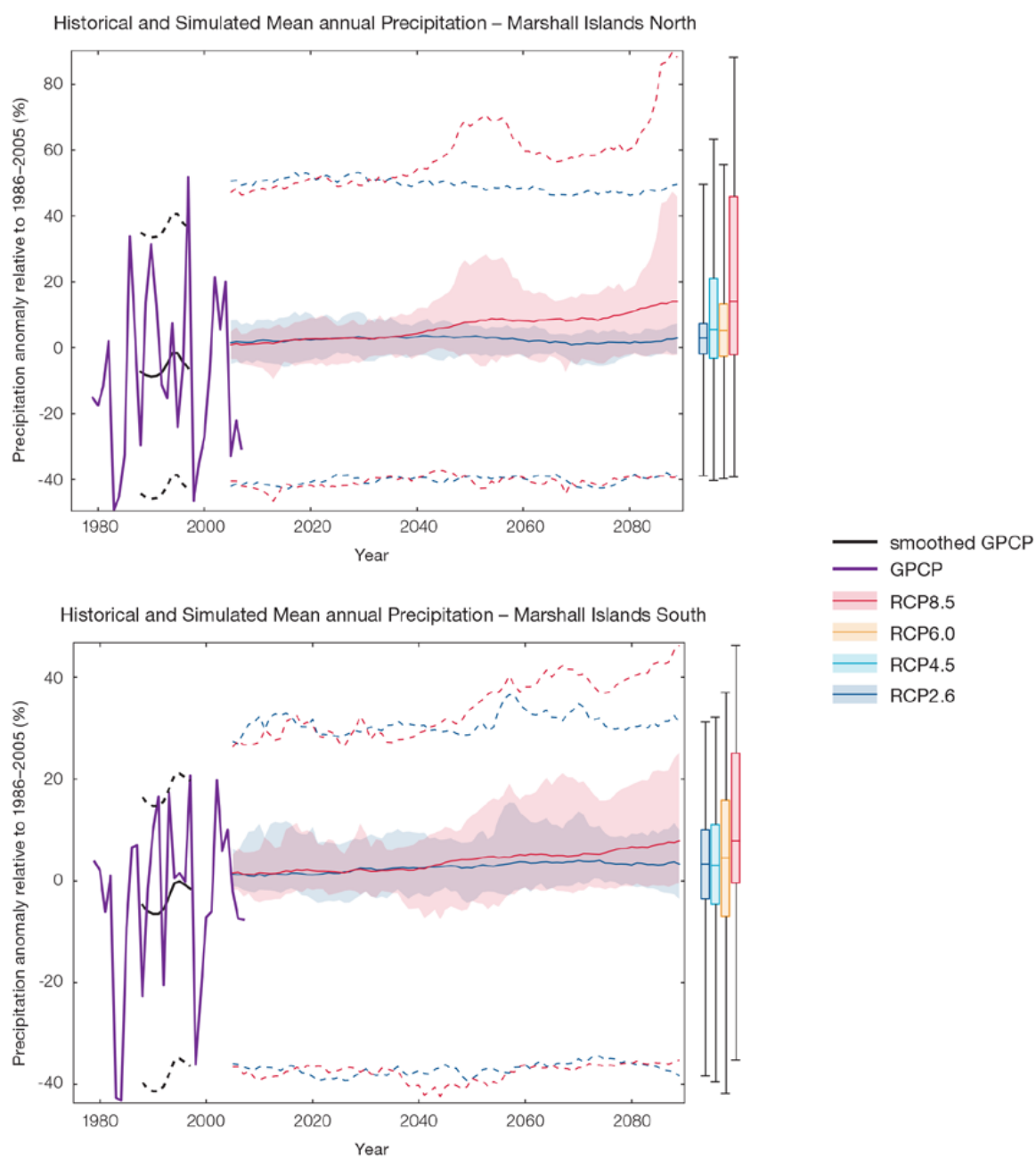


Figure 7.9: Historical and simulated annual average rainfall time series for the region surrounding the northern (top) and southern (bottom) Marshall Islands. The graph shows the anomaly (from the base period 1986–2005) in rainfall from observations (the GPCP dataset, in purple), and for the CMIP5 models under the very high (RCP8.5, in red) and very low (RCP2.6, in blue) emissions scenarios. The solid red and blue lines show the smoothed (20-year running average) multi-model mean anomaly in rainfall, while shading represents the spread of model values (5–95th percentile). The dashed lines show the 5–95th percentile of the observed interannual variability for the observed period (in black) and added to the projections as a visual guide (in red and blue). This indicates that future rainfall could be above or below the projected long-term averages due to interannual variability. The ranges of projections for a 20-year period centred on 2090 are shown by the bars on the right for RCP8.5, 6.0, 4.5 and 2.6.

There is *low confidence* in the magnitude of projected change in extreme temperature because models generally underestimate the current intensity and frequency of extreme events, especially in this area, due to the ‘cold-tongue bias’ (Chapter 1). Changes to the particular driver of extreme temperatures affect whether the change to extremes is more or less than the change in the average temperature, and the changes to the drivers of extreme temperatures in Marshall Islands are currently unclear. Also, while all models project the same direction of change there is a wide range in the projected magnitude of change among the models.

Extreme Rainfall

The frequency and intensity of extreme rainfall events are projected to increase. This conclusion is based on analysis of daily rainfall data from a subset of CMIP5 models using a similar method to that in Australian Bureau of Meteorology and CSIRO (2011) with some improvements (Chapter 1), so the results are slightly different to those in Australian Bureau of Meteorology and CSIRO (2011).

For the northern Marshall Islands current 1-in-20-year daily rainfall amount is projected to increase by approximately 1 mm by 2030 for RCP2.6 and by 7 mm by 2030 for RCP8.5 (very high emissions). By 2090, it is projected to increase by approximately 6 mm for RCP2.6 and by 32 mm for RCP8.5 (very high emissions). The majority of models project the current 1-in-20-year daily rainfall event will become, on average, a 1-in-8-year event for RCP2.6 and a 1-in-5-year event for RCP8.5 (very high emissions) by 2090.

For the southern Marshall Islands the current 1-in-20-year daily rainfall amount is projected to increase by approximately 4 mm by 2030 for RCP2.6 and by 11 mm by 2030 for RCP8.5 (very high emissions).

By 2090, it is projected to increase by approximately 9 mm for RCP2.6 and by 30 mm for RCP8.5 (very high emissions). The majority of models project the current 1-in-20-year daily rainfall event will become, on average, a 1-in-9-year event for RCP2.6 and a 1-in-6-year event for RCP8.5 (very high emissions) by 2090. These results are different to those found in Australian Bureau of Meteorology and CSIRO (2011) because of different methods used (Chapter 1).

There is *high confidence* that the frequency and intensity of extreme rainfall events will increase because:

- A warmer atmosphere can hold more moisture, so there is greater potential for extreme rainfall (IPCC, 2012); and
- Increases in extreme rainfall in the Pacific are projected in all available climate models.

There is *low confidence* in the magnitude of projected change in extreme rainfall because:

- Models generally underestimate the current intensity of local extreme events, especially in this area due to the ‘cold-tongue bias’ (Chapter 1);
- Changes in extreme rainfall projected by models may be underestimated because models seem to underestimate the observed increase in heavy rainfall with warming (Min et al., 2011);
- Global climate models have a coarse spatial resolution, so they do not adequately capture some of the processes involved in extreme rainfall events; and
- The Conformal Cubic Atmospheric Model (CCAM) downscaling model has finer spatial resolution and the CCAM results presented in Australian Bureau of Meteorology and CSIRO (2011) indicates a smaller increase in the number of extreme rainfall days, and there is no clear reason to accept one set of models over another.

Drought

Drought projections (defined in Chapter 1) are described in terms of changes in proportion of time in drought, frequency and duration by 2090 for very low and very high emissions (RCP2.6 and 8.5).

For both the northern and southern Marshall Islands the overall proportion of time spent in drought is expected to decrease under all scenarios. Under RCP8.5 the frequency of drought in all categories is projected to decrease and the duration of events in all drought categories is projected to stay approximately the same (Figure 7.10). Under RCP2.6 (very low emissions) the frequency of moderate, severe and extreme drought is projected to decrease while the frequency of mild drought is projected to remain stable. The duration of events in all categories is projected to stay approximately the same under RCP2.6 (very low emissions).

There is *medium confidence* in this direction of change because:

- There is *high confidence* in the direction of mean rainfall change;
- These drought projections are based upon a subset of models; and
- Like the CMIP3 models, the majority of the CMIP5 models agree on this direction of change.

There is *low confidence* in the projections of drought frequency and duration because there is *medium confidence* in the magnitude of rainfall projections, and no consensus about projected changes in the ENSO, which directly influence the projection of drought.

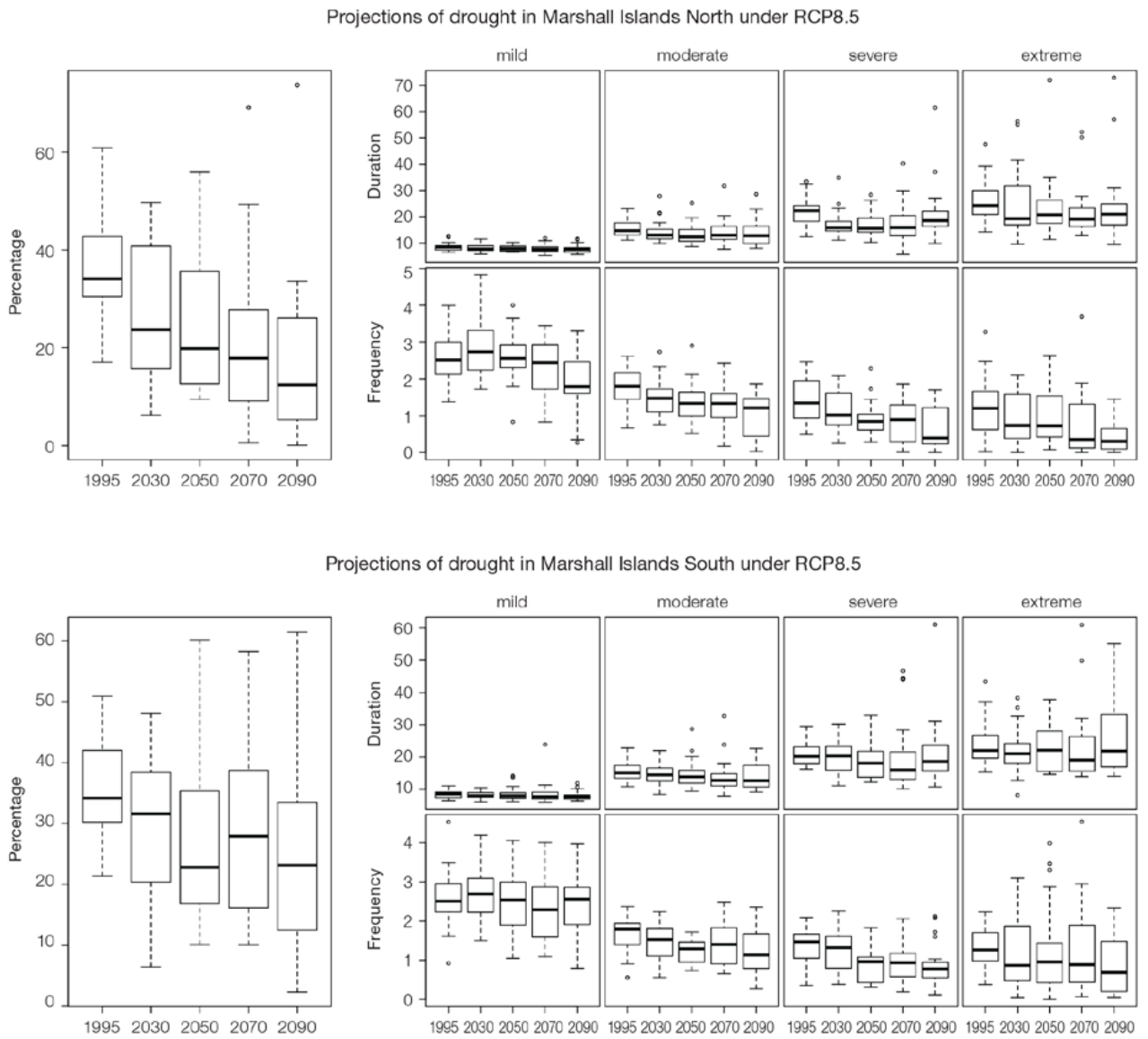


Figure 7.10: Box-plots showing percent of time in moderate, severe or extreme drought (left hand side), and average drought duration and frequency for the different categories of drought (mild, moderate, severe and extreme) for the northern (top) and southern (bottom) Marshall Islands. These are shown for 20-year periods centred on 1995, 2030, 2050, 2070 and 2090 for the RCP8.5 (very high emissions) scenario. The thick dark lines show the median of all models, the box shows the interquartile (25–75%) range, the dashed lines show 1.5 times the interquartile range and circles show outlier results.

Tropical Cyclones

Global Picture

There is a growing level of agreement among models that on a global basis the frequency of tropical cyclones is likely to decrease by the end of the 21st century. The magnitude of the decrease varies from 6%–35% depending on the modelling study. There is also a general agreement between models that there will be an increase in the mean maximum wind speed of cyclones by between 2% and 11% globally, and an increase in rainfall rates of the order of 20% within 100 km of the cyclone centre (Knutson et al., 2010). Thus, the scientific community has a *medium* level of confidence in these global projections.

Marshall Islands

The projection is for a decrease in tropical cyclone genesis (formation) frequency for the northern basin (see Figure 7.11 and Table 7.4). However the confidence level for this projection is low.

The GCMs show inconsistent results across models for changes in tropical cyclone frequency for the northern basin, using either the direct detection methodologies (CVP or CDD) or the empirical methods described in Chapter 1. The direct detection methodologies tend to indicate a decrease in formation with almost half of results suggesting decreases of between 20 and 50%. The empirical techniques assess changes in the main atmospheric ingredients known to be necessary for tropical cyclone formation. About four-fifths of results suggest the conditions for tropical cyclone formation will become more favourable in this region. However, when only the models for which direct detection and empirical methods are available are considered, the assessment is for a decrease in tropical cyclone formation. These projections are consistent with those of Australian Bureau of Meteorology and CSIRO (2011).

Table 7.4: Projected percentage change in cyclone frequency in the northern basin (0–15°N; 130–180°E) for 22 CMIP5 climate models, based on five methods, for 2080–2099 relative to 1980–1999 for RCP8.5 (very high emissions). The 22 CMIP5 climate models were selected based upon the availability of data or on their ability to reproduce a current-climate tropical cyclone climatology (See Section 1.5.3 – Detailed Projection Methods, Tropical Cyclones). Blue numbers indicate projected decreases in tropical cyclone frequency, red numbers an increase. MMM is the multi-model mean change. N increase is the proportion of models (for the individual projection method) projecting an increase in cyclone formation.

Model	GPI change	GPI-M change	Tippett	CDD	OWZ
access10	71	22	-54	71	
access13	55	48	-33	107	
bccscm11	13	11	-22		2
canesm2	34	22	-47	24	
ccsm4				-81	-12
cnrm_cm5	0	-2	-25	-1	-23
csiro_mk36	7	-1	-30	8	15
fgoals_g2	-5	-15	-10		
fgoals_s2	-3	-3	-35		
gfdl-esm2m				-2	-8
gfdl_cm3	15	5	-17		-40
gfdl-esm2g				-33	-37
gisse2r	14	9	-17		
hadgem2_es	13	1	-57		
lnm	25	26	-5		
ipslcm5alr	19	9	-17		
ipslcm5blr				-49	
miroc5				-52	-50
miroc5m	17	2	26		
mpim	19	17	-45		
mrikgcm3	1	-3	-34		
noresm1m	-11	-17	-19	-42	
MMM	17	8	-26	-5	-19
N increase	0.8	0.7	0.1	0.4	0.3

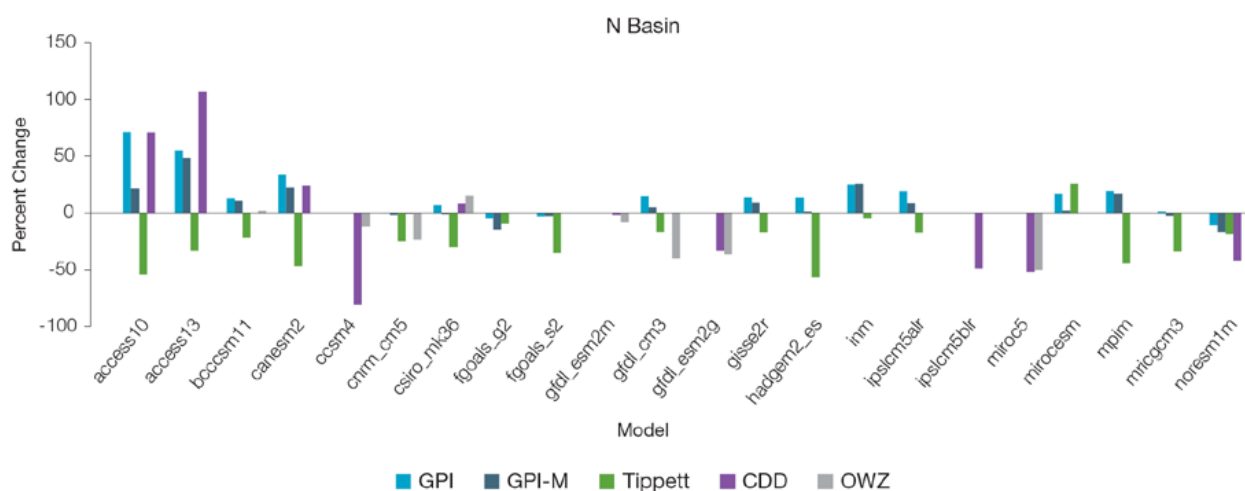


Figure 7.11: Projected percentage change in cyclone frequency in the northern basin (data from Table 7.4).

7.5.4 Coral Reefs and Ocean Acidification

As atmospheric CO₂ concentrations continue to rise, oceans will warm and continue to acidify. These changes will impact the health and viability of marine ecosystems, including coral reefs that provide many key ecosystem services (*high confidence*). These impacts are also likely to be compounded by other stressors such as storm damage, fishing pressure and other human impacts.

The projections for future ocean acidification and coral bleaching use three RCPs (2.6, 4.5, and 8.5).

Ocean Acidification

In the Marshall Islands the aragonite saturation state has declined from about 4.5 in the late 18th century to an observed value of about 3.9±0.1 by 2000 (Kuchinke et al., 2014). All models show that the aragonite saturation state, a proxy for coral reef growth rate, will continue to decrease as atmospheric CO₂ concentrations increase (*very high confidence*). Projections from CMIP5 models indicate that under RCPs 8.5 (very high emissions) and 4.5 (low emissions) the median aragonite saturation state will transition to marginal conditions (3.5) around 2030. In RCP8.5 (very high emissions) the aragonite saturation state continues to strongly decline thereafter to values where coral reefs have not

historically been found (< 3.0). Under RCP4.5 (low emissions) the aragonite saturation plateaus around 3.2 i.e. marginal conditions for healthy coral reefs. While under RCP2.6 (very low emissions) the median aragonite saturation state never falls below 3.5, and increases slightly toward the end of the century (Figure 7.12) suggesting that the conditions remains adequate for healthy coral reefs. There is *medium confidence* in this range and distribution of possible futures because the projections are based on climate models that do not resolve the reef scale that can play a role in modulating large-scale changes. The impacts of ocean acidification are also likely to affect the entire marine ecosystem impacting the key ecosystem services provided by reefs.

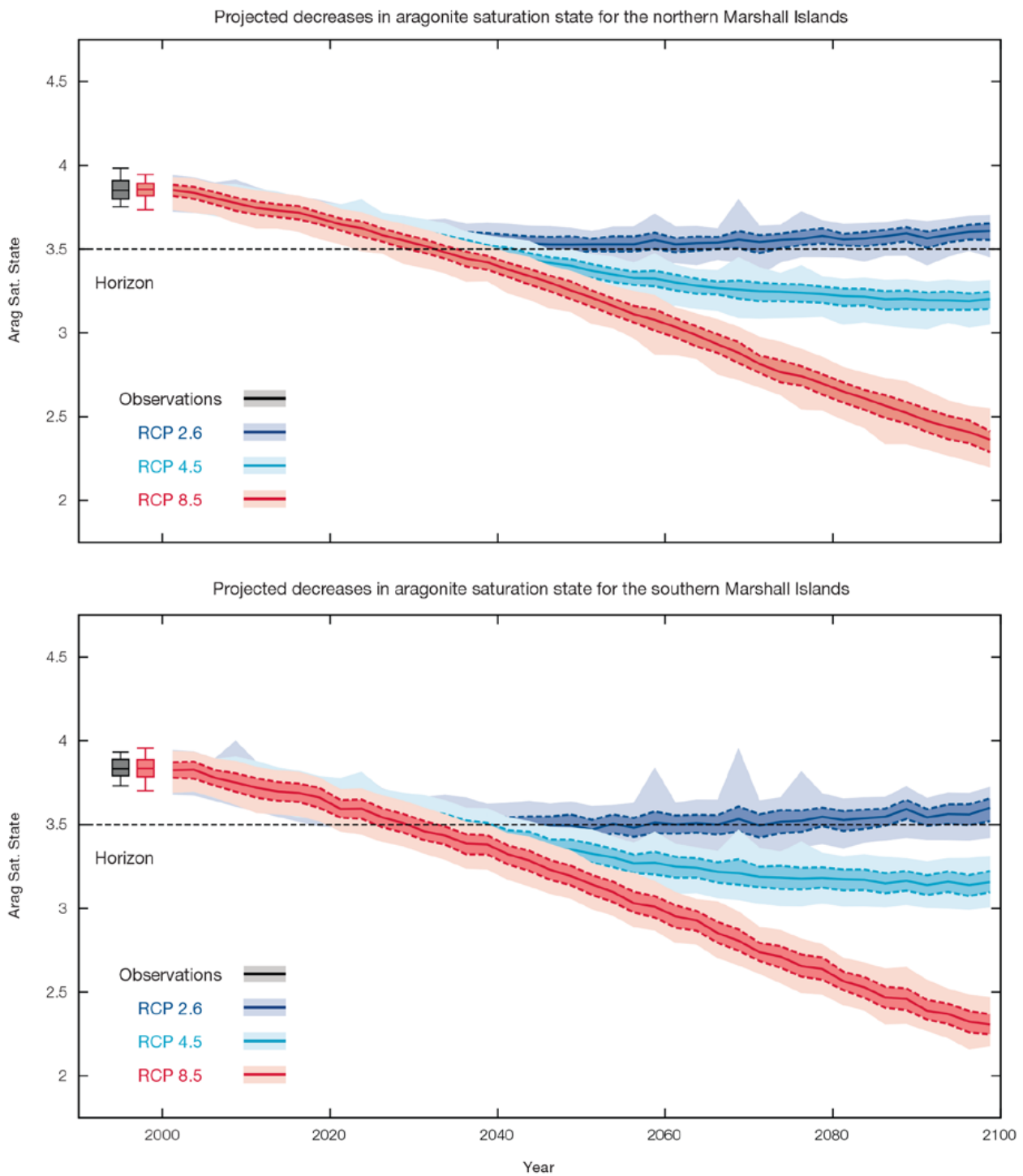


Figure 7.12: Projected decreases in aragonite saturation state in the northern (upper panel) and southern Marshall Islands (lower panel) from CMIP5 models under RCP2.6, 4.5 and 8.5. Shown are the median values (solid lines), the interquartile range (dashed lines), and the 5% and 95% percentiles (light shading). The horizontal line represents the transition to marginal conditions for coral reef health (from Guinotte et al., 2003).

Coral Bleaching Risk

As the ocean warms, the risk of coral bleaching increases (*very high confidence*). There is *medium confidence* in the projected rate of change for the Marshall Islands because there is *medium confidence* in the rate of change of sea-surface temperature (SST), and the changes at the reef scale (which can play a role in modulating large-scale changes) are not adequately resolved. Importantly, the coral bleaching risk calculation does not account the impact of other potential stressors (Chapter 1).

The changes in the frequency (or recurrence) and duration of severe bleaching risk are quantified for different projected SST changes (Table 7.5). Overall there is a decrease in the time between two periods of

elevated risk and an increase in the duration of the elevated risk. For example, under a long-term mean increase of 1°C (relative to 1982–1999 period), the average period of severe bleaching risk (referred to as a risk event) will last 8.9 weeks (with a minimum duration of 2.5 weeks and a maximum duration of 3.5 months) and the average time between two risks will be 3.3 years (with the minimum recurrence of 8.3 months and a maximum recurrence of 10.0 years). If severe bleaching events occur more often than once every five years, the long-term viability of coral reef ecosystems becomes threatened.

7.5.5 Sea Level

Mean sea level is projected to continue to rise over the course of the 21st century. There is *very high confidence* in the direction of change. The CMIP5 models simulate a rise of between approximately 7–19 cm by 2030 (very similar values for different RCPs), with increases of 41–92 cm by 2090 under the RCP8.5 (Figure 7.13 and Tables 7.6 and 7.7). There is *medium confidence* in the range mainly because there is still uncertainty associated with projections of the Antarctic ice sheet contribution. Interannual variability of sea level will lead to periods of lower and higher regional sea levels. In the past, this interannual variability has been about 20 cm (5–95% range, after removal of the seasonal signal, see dashed lines in Figure 7.13 (a) and it is likely that a similar range will continue through the 21st century.

Table 7.5: Projected changes in severe coral bleaching risk for the Marshall Islands EEZ for increases in SST relative to 1982–1999.

Temperature change ¹	Recurrence interval ²	Duration of the risk event ³
Change in observed mean	0	0
+0.25°C	30 years	3.5 weeks
+0.5°C	28.0 years (27.3 years – 28.7 years)	5.4 weeks (5.2 weeks – 5.6 weeks)
+0.75°C	13.8 years (9.0 years – 19.5 years)	6.4 weeks (4.2 weeks – 8.8 weeks)
+1°C	3.3 years (8.3 months – 10.0 years)	8.9 weeks (2.5 weeks – 3.5 months)
+1.5°C	9.6 months (3.4 months – 2.5 years)	4.1 months (3.0 weeks – 7.4 months)
+2°C	5.1 months (2.3 months – 8.3 months)	7.3 months (8.5 weeks – 1.6 years)

¹ This refers to projected SST anomalies above the mean for 1982–1999.

² Recurrence is the mean time between severe coral bleaching risk events. Range (min – max) shown in brackets.

³ Duration refers to the period of time where coral are exposed to the risk of severe bleaching. Range (min – max) shown in brackets.

Observed and projected relative sea-level change near the Marshall Islands

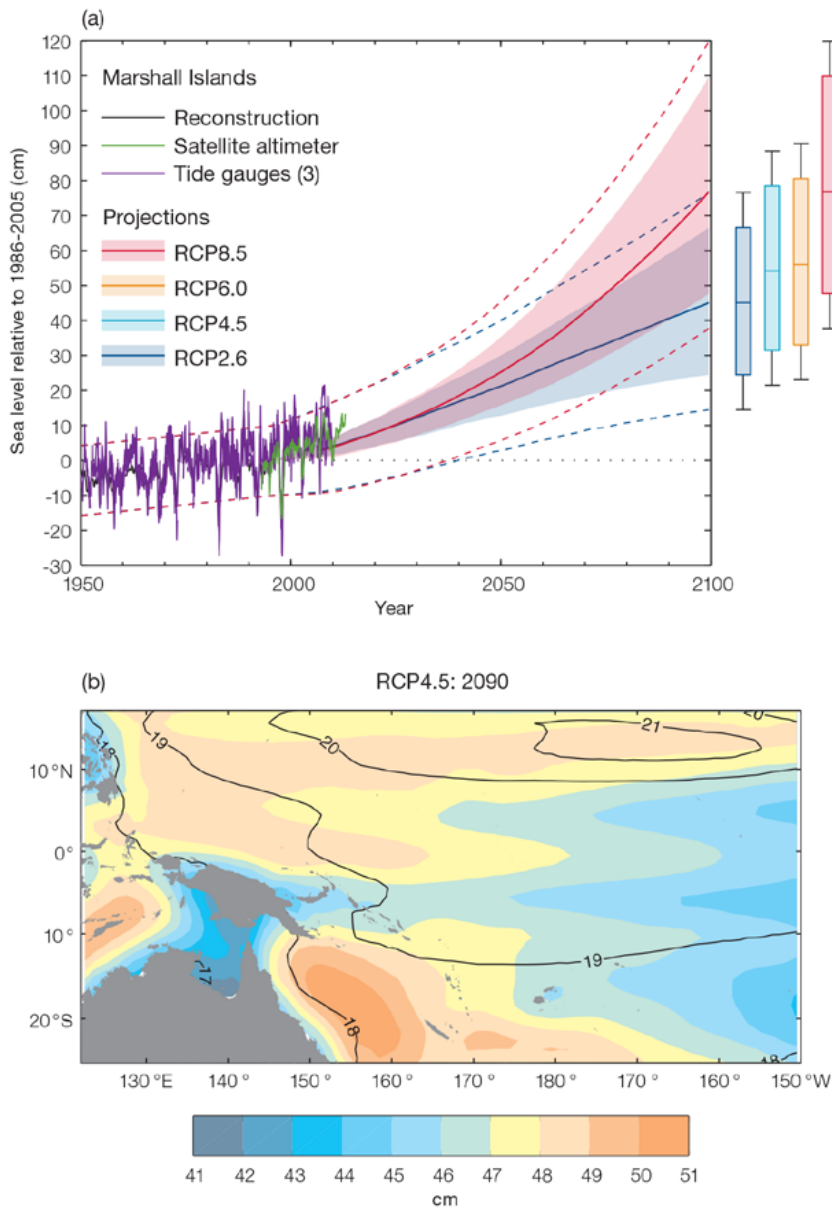


Figure 7.13: (a) The observed tide-gauge records of relative sea-level (since the late 1970s) are indicated in purple, and the satellite record (since 1993) in green. The gridded (reconstructed) sea level data at the Marshall Islands (since 1950) is shown in black. Multi-model mean projections from 1995–2100 are given for the RCP8.5 (red solid line) and RCP2.6 emissions scenarios (blue solid line), with the 5–95% uncertainty range shown by the red and blue shaded regions. The ranges of projections for four emission scenarios (RCPs 2.6, 4.5, 6.0 and 8.5) by 2100 are also shown by the bars on the right. The dashed lines are an estimate of interannual variability in sea level (5–95% uncertainty range about the projections) and indicate that individual monthly averages of sea level can be above or below longer-term averages.

(b) The regional distribution of projected sea level rise under the RCP4.5 emissions scenario for 2081–2100 relative to 1986–2005. Mean projected changes are indicated by the shading, and the estimated uncertainty in the projections is indicated by the contours (in cm).

7.5.6 Wind-driven Waves

The projected changes in wave climate vary across the Marshall Islands.

In the northern Marshall Islands, there is a projected decrease in December–March wave height (significant under RCP8.5, very high emissions, by 2090 across the season, and also in February under RCP4.5 in 2035 and 2090, and March under RCP8.5, very high emissions, in 2035 and RCP4.5 in 2090) (Figure 7.14) consistent with a decrease in northern trade winds, with a suggested decrease in wave period, and no change in direction (*low confidence*) (Table 7.8). In the wet season (June–September) there is no projected change in wave height or period but a strong clockwise rotation toward the south is suggested under RCP8.5, very high emissions, in 2090 and in all scenarios in September, possibly as a result of increased projected numbers of westerly and south-westerly waves from monsoons or typhoons, or southern storm swell (*low confidence*). Storm wave heights are projected to decrease by around 1' (30 cm) by the end of the 21st century in December–March (*low confidence*).

In the southern Marshall Islands, projected changes in wave properties include a decrease in wave height (significant in January–March under RCP8.5, very high emissions, by 2090, in February under RCP4.5 in 2090 and in March in all scenarios except RCP4.5 in 2035) (Figure 7.15) consistent with a decrease in northern trade winds, with an associated decrease in wave period and no change in direction during the December–March dry season (*low confidence*) (Table 7.9). During

June–September, no significant changes are projected to occur in wave height or period (*low confidence*), while a large but non-significant clockwise rotation of direction is projected by 2090, due to more southerly and south-westerly waves resulting from monsoons or typhoons, or perhaps swell from southern storms (*very low confidence*). A decrease in the height of storm waves by around 8” (20 cm) is suggested in the dry season (*low confidence*).

There is *low confidence* in projected changes in the Marshall Islands wind-wave climate because:

- Projected changes in wave climate are dependent on confidence in projected changes in the ENSO, which is low; and
- The differences between simulated and observed (hindcast) wave data can be larger than the projected wave changes, which further reduces our confidence in projections.

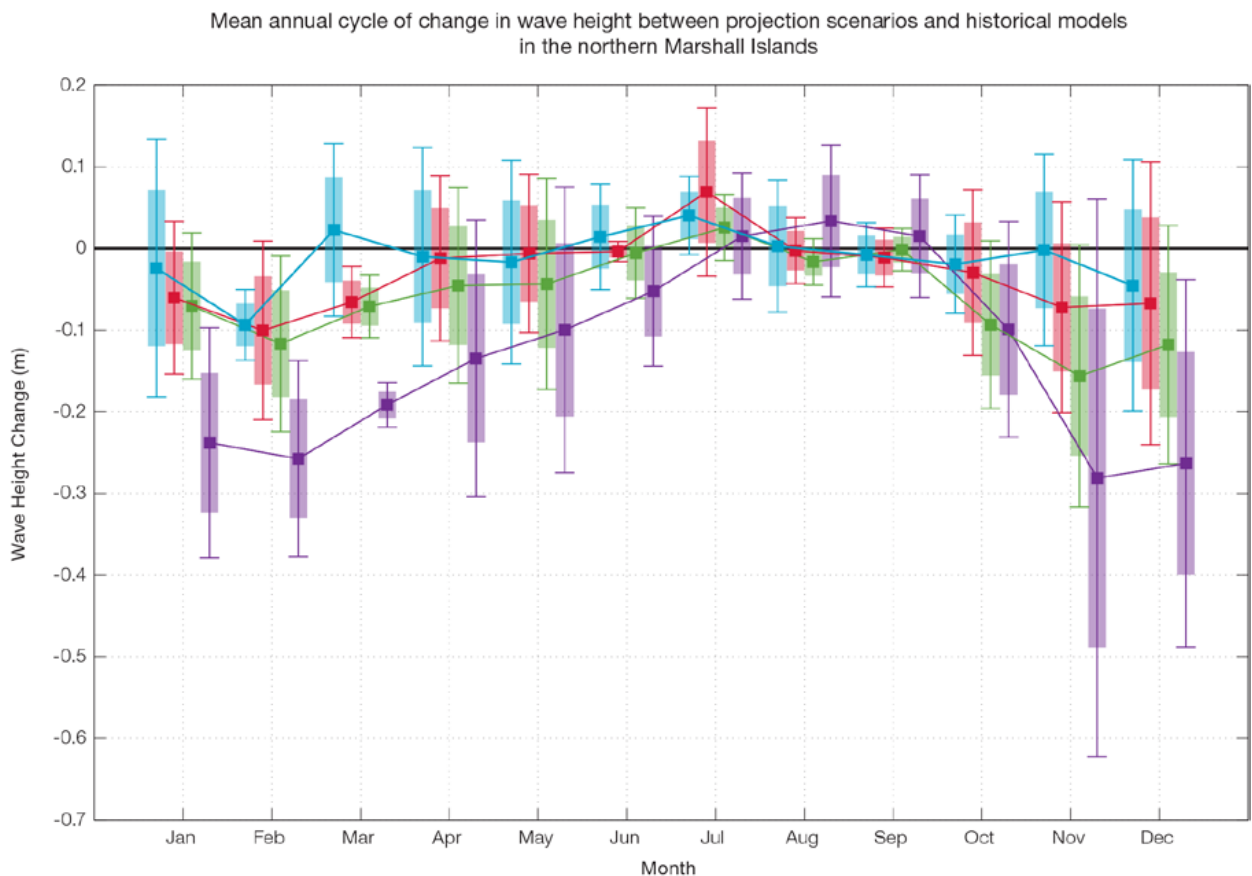


Figure 7.14: Mean annual cycle of change in wave height between projection scenarios and historical models in the northern Marshall Islands. This plot shows a decrease in wave heights in November–March, and no change in June–September. Shaded boxes show 1 standard deviation of models’ means around the ensemble means, and error bars show the 5–95% range inferred from the standard deviation. Colours represent RCP scenarios and time periods: blue 2035 RCP4.5 (low emissions), red 2035 RCP8.5 (very high emissions), green 2090 RCP4.5 (low emissions), purple 2090 RCP8.5 (very high emissions).

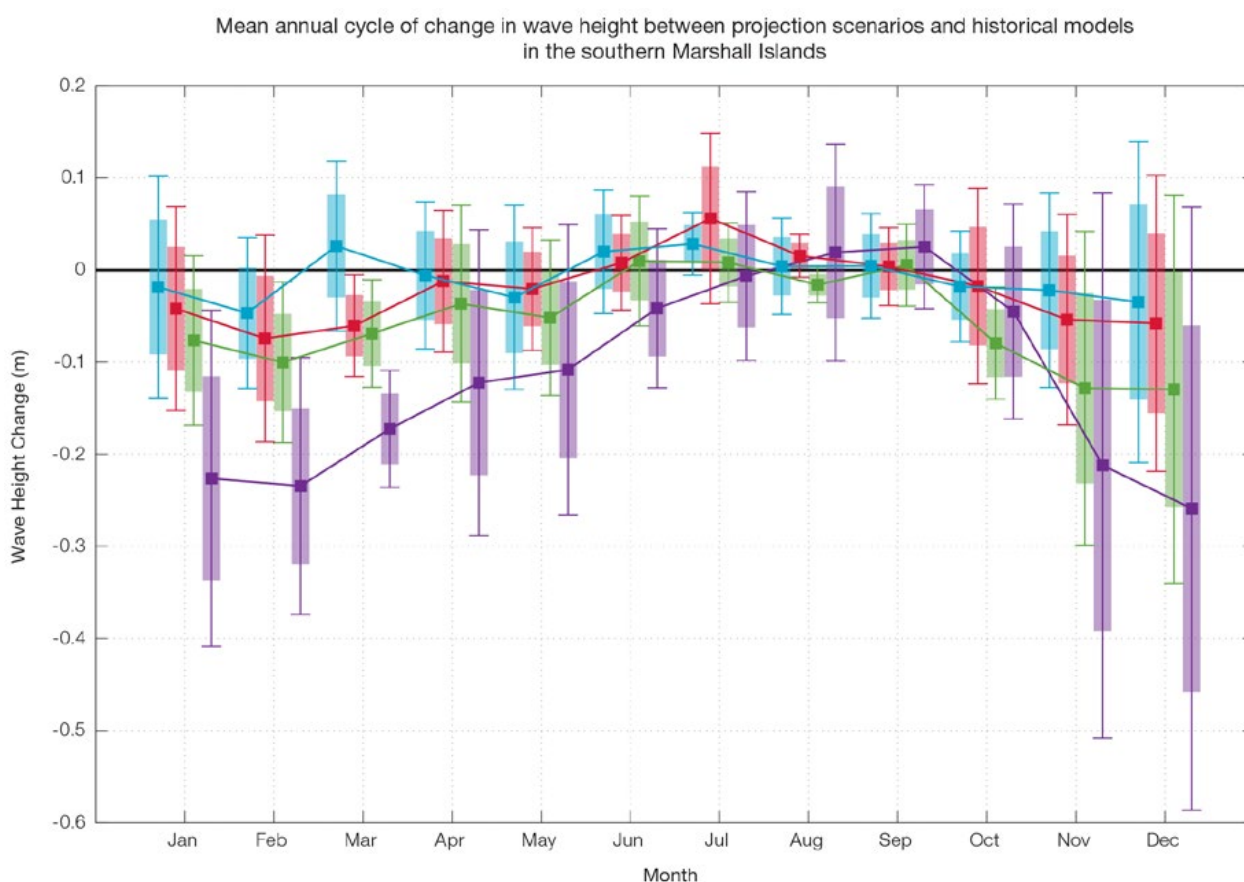


Figure 7.15: Mean annual cycle of change in wave height between projection scenarios and historical models in the southern Marshall Islands. This figure shows a decrease in wave heights in November–March (significant in January–March in some scenarios), and no significant change in June–September. Shaded boxes show 1 standard deviation of models’ means around the ensemble means, and error bars show the 5–95% range inferred from the standard deviation. Colours represent RCP scenarios and time periods: blue 2035 RCP4.5 (low emissions), red 2035 RCP8.5 (very high emissions), green 2090 RCP4.5 (low emissions), purple 2090 RCP8.5 (very high emissions).

7.5.7 Projections Summary

There is *very high confidence* in the direction of long-term change in a number of key climate variables, namely an increase in mean and extremely high temperatures, sea level and ocean acidification. There is *high confidence* that the frequency and intensity of extreme rainfall will increase. There is *high confidence* that mean rainfall will increase, and

medium confidence in a decrease in drought frequency.

Tables 7.6–7.9 quantify the mean changes and ranges of uncertainty for a number of variables, years and emissions scenarios. A number of factors are considered in assessing confidence, i.e. the type, amount, quality and consistency of evidence (e.g. mechanistic understanding, theory, data, models, expert judgment) and the degree of agreement, following

the IPCC guidelines (Mastrandrea et al., 2010). Confidence ratings in the projected magnitude of mean change are generally lower than those for the direction of change (see paragraph above) because magnitude of change is more difficult to assess. For example, there is *very high confidence* that temperature will increase, but *medium confidence* in the magnitude of mean change.

Table 7.6: Projected changes in the annual and seasonal mean climate for the northern Marshall Islands under four emissions scenarios; RCP2.6 (very low emissions, in dark blue), RCP4.5 (low emissions, in light blue), RCP6 (medium emissions, in orange) and RCP8.5 (very high emissions, in red). Projected changes are given for four 20-year periods centred on 2030, 2050, 2070 and 2090, relative to a 20-year period centred on 1995. Values represent the multi-model mean change, with the 5–95% range of uncertainty in brackets. Confidence in the magnitude of change is expressed as *high*, *medium* or *low*. Surface air temperatures in the Pacific are closely related to sea-surface temperatures (SST), so the projected changes to air temperature given in this table can be used as a guide to the expected changes to SST. (See also Section 1.5.2). ‘NA’ indicates where data are not available.

Variable	Season	2030	2050	2070	2090	Confidence (magnitude of change)
Surface air temperature (°C)	Annual	0.7 (0.5 to 1)	0.8 (0.6 to 1.2)	0.8 (0.5 to 1.2)	0.8 (0.5 to 1.2)	<i>Medium</i>
		0.7 (0.4 to 1)	1.1 (0.7 to 1.4)	1.4 (0.9 to 1.9)	1.5 (1 to 2.1)	
		0.6 (0.4 to 0.9)	1 (0.7 to 1.4)	1.4 (1.1 to 2)	1.9 (1.4 to 2.6)	
		0.8 (0.5 to 1.1)	1.5 (1 to 1.9)	2.2 (1.6 to 3.2)	3.1 (2.2 to 4.2)	
Maximum temperature (°C)	1-in-20 year event	0.7 (0.4 to 1.1)	0.8 (0.4 to 1.3)	0.8 (0.2 to 1)	0.8 (0.4 to 1.2)	<i>Medium</i>
		0.7 (0.3 to 1)	1 (0.6 to 1.4)	1.3 (0.6 to 2)	1.4 (0.8 to 2)	
		NA (NA to NA)				
		0.8 (0.4 to 1.2)	1.6 (0.9 to 2.2)	2.4 (1.4 to 3.5)	3.3 (1.9 to 4.4)	
Minimum temperature (°C)	1-in-20 year event	0.7 (0.4 to 1)	0.9 (0.5 to 1.3)	0.9 (0.4 to 1.2)	0.9 (0.2 to 1.3)	<i>Medium</i>
		0.7 (0.1 to 1.1)	1.1 (0.7 to 1.4)	1.4 (0.9 to 1.9)	1.5 (0.8 to 2)	
		NA (NA to NA)				
		0.9 (0.3 to 1.2)	1.7 (0.9 to 2.3)	2.4 (1.5 to 3.3)	3.4 (1.9 to 4.7)	
Total rainfall (%)	Annual	3 (-2 to 11)	3 (-2 to 8)	1 (-4 to 4)	3 (-2 to 7)	<i>Medium</i>
		2 (-6 to 7)	4 (-7 to 15)	7 (-2 to 10)	5 (-3 to 21)	
		1 (-6 to 8)	4 (0 to 7)	6 (-1 to 13)	5 (-3 to 13)	
		3 (-5 to 7)	8 (-2 to 26)	8 (-4 to 16)	14 (-2 to 46)	
Total rainfall (%)	Nov-Apr	6 (-6 to 18)	8 (-4 to 18)	7 (-7 to 18)	4 (-9 to 13)	<i>Medium</i>
		2 (-8 to 16)	6 (-7 to 24)	11 (-2 to 29)	8 (-5 to 26)	
		0 (-9 to 14)	7 (-5 to 18)	11 (0 to 23)	12 (-1 to 27)	
		5 (-8 to 15)	10 (-4 to 29)	11 (-5 to 26)	18 (-4 to 52)	
Total rainfall (%)	May-Oct	2 (-5 to 11)	2 (-3 to 6)	-1 (-7 to 3)	3 (-2 to 7)	<i>Medium</i>
		2 (-5 to 8)	4 (-6 to 19)	5 (-2 to 10)	4 (-6 to 21)	
		1 (-6 to 8)	3 (-1 to 7)	4 (-5 to 12)	3 (-7 to 12)	
		2 (-3 to 10)	7 (-3 to 26)	8 (-7 to 13)	13 (-6 to 44)	
Aragonite saturation state (Ω_{ar})	Annual	-0.3 (-0.6 to -0.1)	-0.4 (-0.7 to -0.1)	-0.4 (-0.6 to -0.1)	-0.3 (-0.6 to -0.1)	<i>Medium</i>
		-0.3 (-0.6 to -0.1)	-0.5 (-0.8 to -0.3)	-0.7 (-0.9 to -0.5)	-0.7 (-1.0 to -0.5)	
		NA (NA to NA)				
		-0.4 (-0.6 to -0.1)	-0.7 (-0.9 to -0.5)	-1.1 (-1.3 to -0.9)	-1.5 (-1.7 to -1.3)	
Mean sea level (cm)	Annual	13 (7 to 18)	22 (13 to 30)	31 (19 to 45)	41 (23 to 60)	<i>Medium</i>
		12 (7 to 18)	23 (14 to 32)	35 (21 to 49)	48 (28 to 69)	
		12 (7 to 17)	22 (14 to 31)	35 (21 to 49)	49 (30 to 70)	
		13 (8 to 19)	26 (16 to 35)	43 (27 to 60)	65 (41 to 92)	

Table 7.7: Projected changes in the annual and seasonal mean climate for the southern Marshall Islands under four emissions scenarios; RCP2.6 (very low emissions, in dark blue), RCP4.5 (low emissions, in light blue), RCP6 (medium emissions, in orange) and RCP8.5 (very high emissions, in red). Projected changes are given for four 20-year periods centred on 2030, 2050, 2070 and 2090, relative to a 20-year period centred on 1995. Values represent the multi-model mean change, with the 5–95% range of uncertainty in brackets. Confidence in the magnitude of change is expressed as *high*, *medium* or *low*. Surface air temperatures in the Pacific are closely related to sea-surface temperatures (SST), so the projected changes to air temperature given in this table can be used as a guide to the expected changes to SST. (See also Section 1.5.2). ‘NA’ indicates where data are not available.

Variable	Season	2030	2050	2070	2090	Confidence (magnitude of change)
Surface air temperature (°C)	Annual	0.7 (0.4 to 0.9)	0.8 (0.6 to 1.2)	0.8 (0.5 to 1.2)	0.8 (0.5 to 1.2)	<i>Medium</i>
		0.7 (0.5 to 1)	1.1 (0.7 to 1.4)	1.4 (1 to 1.8)	1.5 (1 to 2.1)	
		0.6 (0.4 to 0.9)	1 (0.7 to 1.4)	1.4 (1 to 2)	1.8 (1.3 to 2.6)	
		0.8 (0.6 to 1.1)	1.4 (1 to 1.9)	2.2 (1.7 to 3.1)	3 (2.1 to 4)	
Maximum temperature (°C)	1-in-20 year event	0.7 (0.3 to 1.2)	0.8 (0.3 to 1.4)	0.8 (0.2 to 1.1)	0.8 (0.5 to 1.1)	<i>Medium</i>
		0.6 (0.3 to 1)	0.9 (0.5 to 1.4)	1.2 (0.7 to 1.7)	1.4 (0.9 to 2)	
		NA (NA to NA)				
		0.8 (0.4 to 1.1)	1.5 (0.9 to 2.1)	2.3 (1.3 to 3.4)	3.1 (2 to 4.3)	
Minimum temperature (°C)	1-in-20 year event	0.6 (0.4 to 1)	0.8 (0.3 to 1.2)	0.8 (0.2 to 1.1)	0.8 (0.3 to 1.1)	<i>Medium</i>
		0.7 (0.4 to 1)	1 (0.6 to 1.4)	1.3 (0.8 to 1.8)	1.4 (1 to 1.8)	
		NA (NA to NA)				
		0.8 (0.5 to 1.1)	1.5 (0.8 to 2.1)	2.4 (1.6 to 3.2)	3.2 (2.3 to 4.2)	
Total rainfall (%)	Annual	2 (-3 to 8)	3 (-4 to 8)	4 (-1 to 12)	3 (-4 to 10)	<i>Medium</i>
		1 (-4 to 5)	3 (-3 to 8)	4 (-2 to 10)	3 (-5 to 11)	
		1 (-2 to 5)	2 (-2 to 11)	4 (-5 to 13)	5 (-7 to 16)	
		2 (-3 to 11)	4 (-6 to 12)	5 (-3 to 20)	8 (0 to 25)	
Total rainfall (%)	Nov-Apr	2 (-4 to 9)	3 (-7 to 13)	4 (-5 to 15)	3 (-10 to 12)	<i>Medium</i>
		1 (-7 to 11)	2 (-9 to 14)	4 (-9 to 17)	2 (-11 to 14)	
		0 (-5 to 5)	2 (-7 to 12)	3 (-9 to 14)	3 (-10 to 15)	
		2 (-6 to 9)	4 (-7 to 14)	2 (-13 to 16)	5 (-11 to 31)	
Total rainfall (%)	May-Oct	3 (-2 to 11)	3 (-5 to 9)	3 (0 to 8)	4 (-1 to 12)	<i>Medium</i>
		2 (-4 to 6)	4 (-3 to 9)	5 (-5 to 13)	5 (-5 to 16)	
		2 (-1 to 6)	3 (-5 to 12)	5 (-6 to 16)	6 (-7 to 19)	
		3 (-1 to 8)	5 (-5 to 13)	8 (-6 to 17)	11 (-6 to 26)	
Aragonite saturation state (Ωar)	Annual	-0.3 (-0.6 to 0.0)	-0.4 (-0.7 to -0.1)	-0.4 (-0.7 to -0.1)	-0.3 (-0.6 to -0.0)	<i>Medium</i>
		-0.3 (-0.6 to 0.0)	-0.5 (-0.8 to -0.2)	-0.6 (-0.9 to -0.4)	-0.7 (-1.0 to -0.4)	
		NA (NA to NA)				
		-0.4 (-0.7 to -0.1)	-0.7 (-1.0 to -0.4)	-1.1 (-1.3 to -0.8)	-1.4 (-1.7 to -1.1)	
Mean sea level (cm)	Annual	13 (7 to 18)	22 (13 to 30)	31 (19 to 45)	41 (23 to 60)	<i>Medium</i>
		12 (7 to 18)	23 (14 to 32)	35 (21 to 49)	48 (28 to 69)	
		12 (7 to 17)	22 (14 to 31)	35 (21 to 49)	49 (30 to 70)	
		13 (8 to 19)	26 (16 to 35)	43 (27 to 60)	65 (41 to 92)	

Waves Projections Summary

Table 7.8: Projected average changes in wave height, period and direction in the northern Marshall Islands for December–March and June–September for RCP4.5 (low emissions, in blue) and RCP8.5 (very high emissions, in red), for two 20-year periods (2026–2045 and 2081–2100), relative to a 1986–2005 historical period. The values in brackets represent the 5th to 95th percentile range of uncertainty.

Variable	Season	2035	2090	Confidence (range)
Wave height change (m)	December–March	-0.0 (-0.2 to 0.2) -0.1 (-0.3 to 0.1)	-0.1 (-0.3 to 0.1) -0.2 (-0.5 to 0.0)	Low
	June–September	+0.0 (-0.2 to 0.2) +0.0 (-0.2 to 0.2)	0.0 (-0.2 to 0.2) 0.0 (-0.2 to 0.2)	Low
Wave height change (ft)	December–March	-0.1 (-0.8 to 0.7) -0.2 (-1.0 to 0.5)	-0.3 (-1.1 to 0.4) -0.8 (-1.5 to 0.1)	Low
	June–September	+0.0 (-0.6 to 0.6) +0.0 (-0.6 to 0.6)	0.0 (-0.6 to 0.7) 0.0 (-0.6 to 0.8)	Low
Wave period change (s)	December–March	-0.1 (-0.6 to 0.5) -0.1 (-0.6 to 0.5)	-0.1 (-0.8 to 0.5) -0.2 (-1.0 to 0.5)	Low
	June–September	-0.0 (-0.9 to 0.8) -0.1 (-0.9 to 0.7)	-0.0 (-0.9 to 0.9) -0.0 (-0.9 to 0.8)	Low
Wave direction change (° clockwise)	December–March	0 (-10 to 10) 0 (-10 to 10)	0 (-10 to 10) -0 (-10 to 10)	Low
	June–September	0 (-10 to 10) +0 (-10 to 20)	+0 (-10 to 20) +10 (-10 to 30)	Low

Table 7.9: Projected average changes in wave height, period and direction in the southern Marshall Islands for December–March and June–September for RCP4.5 (low emissions, in blue) and RCP8.5 (very high emissions, in red), for two 20-year periods (2026–2045 and 2081–2100), relative to a 1986–2005 historical period. The values in brackets represent the 5th to 95th percentile range of uncertainty.

Variable	Season	2035	2090	Confidence (range)
Wave height change (m)	December–March	-0.0 (-0.3 to 0.2) -0.1 (-0.3 to 0.2)	-0.1 (-0.3 to 0.1) -0.2 (-0.4 to 0.0)	Low
	June–September	0.0 (-0.2 to 0.2) +0.0 (-0.2 to 0.2)	0.0 (-0.2 to 0.2) 0.0 (-0.1 to 0.1)	Low
Wave height change (ft)	December–March	-0.1 (-0.9 to 0.7) -0.2 (-1.0 to 0.7)	-0.3 (-1.1 to 0.4) -0.7 (-1.4 to 0.1)	Low
	June–September	+0.0 (-0.5 to 0.7) +0.1 (-0.5 to 0.7)	0.0 (-0.6 to 0.6) 0.0 (-0.3 to 0.5)	Low
Wave period change (s)	December–March	-0.1 (-0.7 to 0.7) -0.1 (-0.7 to 0.8)	-0.1 (-0.8 to 0.8) -0.2 (-1.0 to 0.8)	Low
	June–September	0.0 (-0.9 to 0.9) -0.1 (-0.9 to 0.8)	0.0 (-0.9 to 0.9) -0.0 (-0.8 to 0.8)	Low
Wave direction change (° clockwise)	December–March	0 (-10 to 10) 0 (-10 to 10)	0 (-10 to 10) -0 (-10 to 10)	Low
	June–September	0 (-20 to 20) 0 (-20 to 20)	+0 (-20 to 30) +10 (-20 to 40)	Low

Wind-wave variables parameters are calculated for a 20-year period centred on 2035.